Statistical analysis of neutral winds in the MLT using 14 years (2007–2020) of meteor radar data at King Sejong Station

Byeong-Gwon Song[1], Changsup Lee[1], Jeong-Han Kim[1], In-Sun Song[1], Geonhwa Jee[1], and Hye-Yeong Chun[2]

[1]Division of Polar Climate Research, Korea Polar Research Institute, South Korea
[2]Department of Atmospheric Sciences, Yonsei University, South Korea

Introduction

- **The mesosphere and lower thermosphere** (**MLT**) **region** is an important region connecting the lower atmosphere and the space.
- Investigation of atmospheric dynamics in the MLT region, therefore, is essential to understand a coupling process between the lower atmosphere and the space.
- **A meteor radar (MR)** can continuously observe **winds** and temperatures in the MLT region regardless of weather conditions.
- MLT winds over **King Sejong Station (KSS)** have been observed using the very high frequency MR since March 2007.
- The observed horizontal winds consist of large-scale components, including **atmospheric tides** (such as semidiurnal tides and diurnal tides) and **planetary waves (PWs)** (such as 2-, and 4-day waves).
- A study on the temporal characteristics of the neutral winds and waves revealed from the long-term observations will improve our understanding of wave dynamics and vertical couplings between the lower and upper atmosphere.

In this study, we investigate the seasonal, interannual, and long-term **variability** of the **neutral winds** including **tide and PW components** in the **MLT** at KSS using the **MR** for 14 years (2007–2020).

Data and Methodology

❖ Meteor radar data at KSS

Meteor radar at KSS		
Variables		U and V
Period		Mar. 2007–Sep. 2020 (~14 years)
Resolution	Temporal	1 hour (sampling: every 2 min)
	Vertical	Six height gates with representative heights of 81.1, 84.6, 87.5, 90.5, 93.3, and 96.8 km

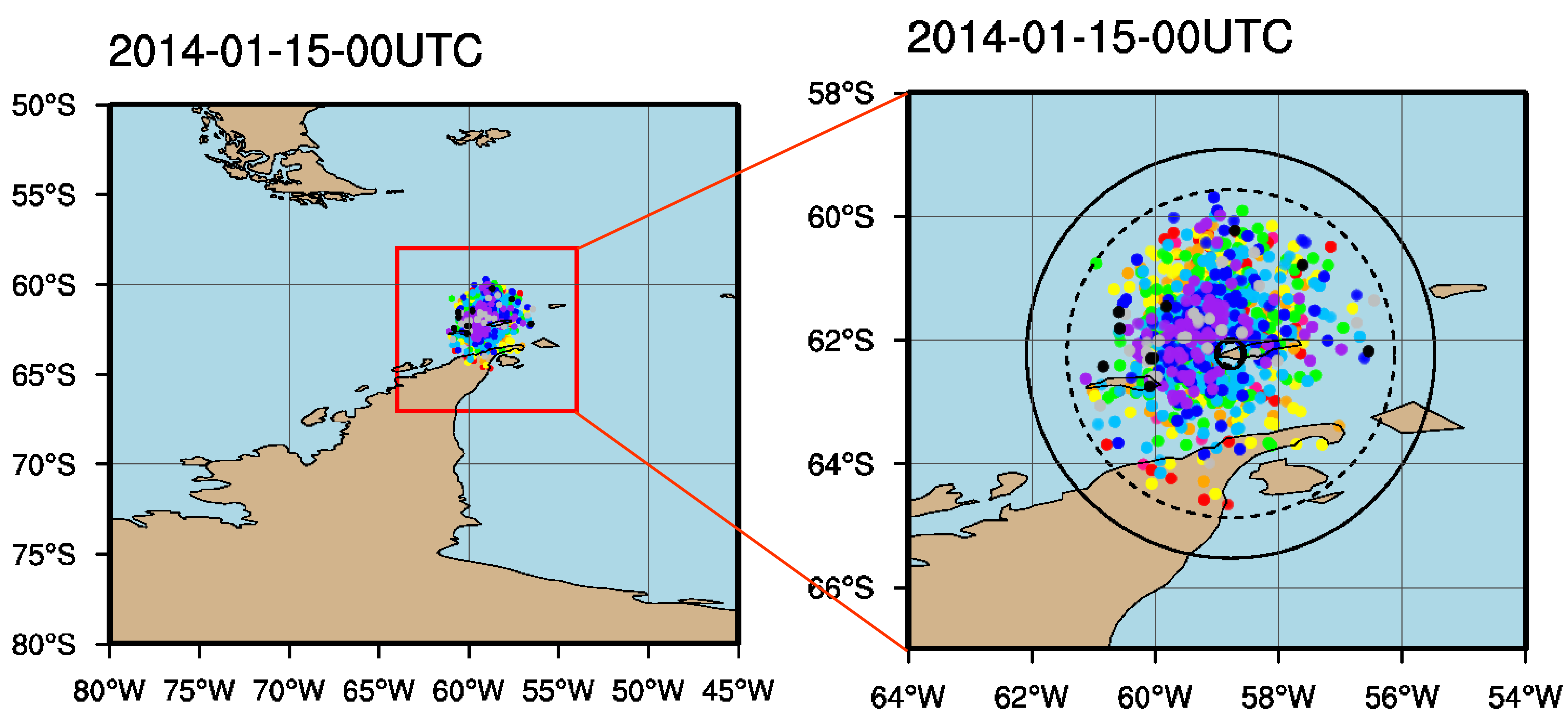

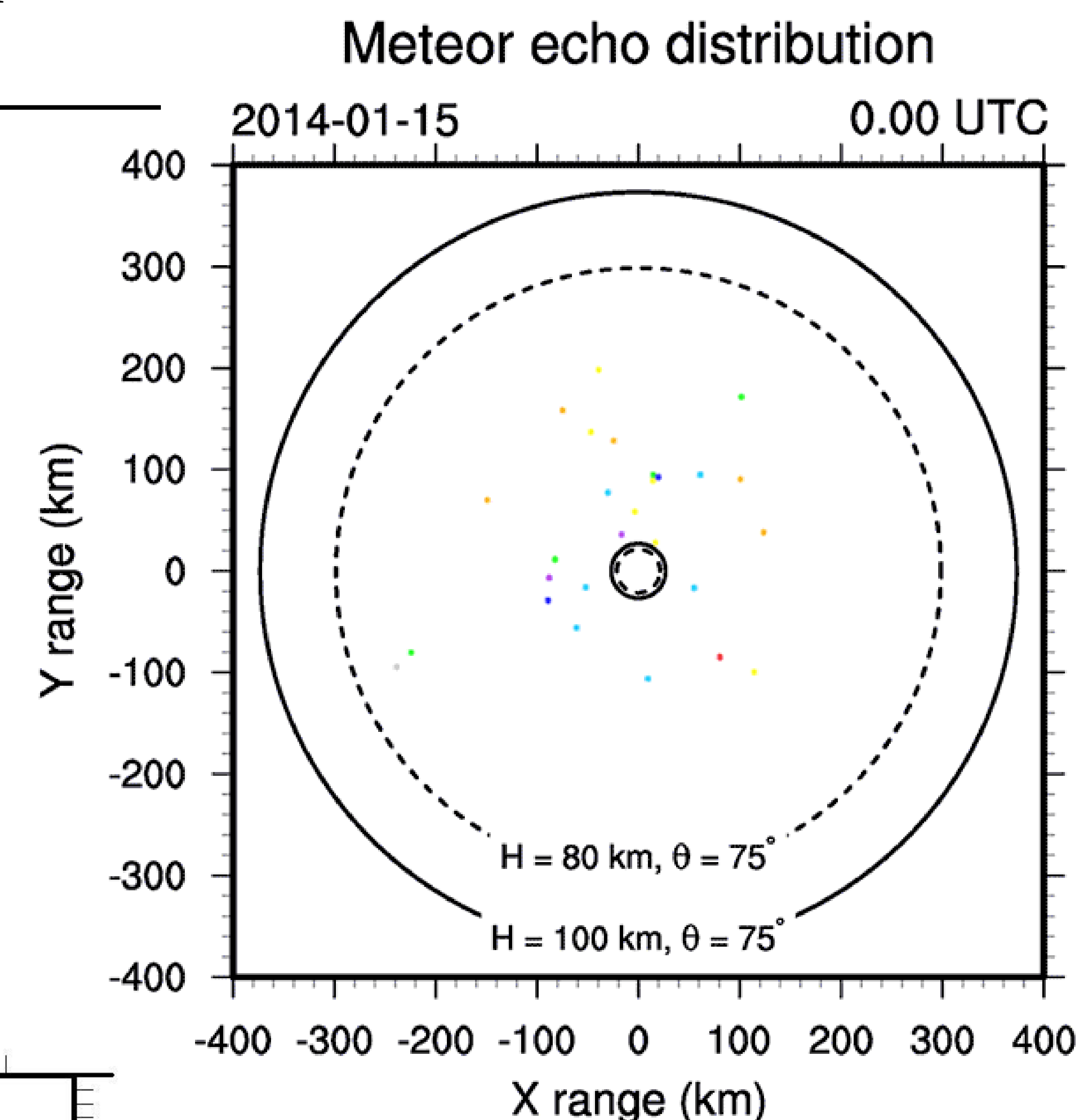

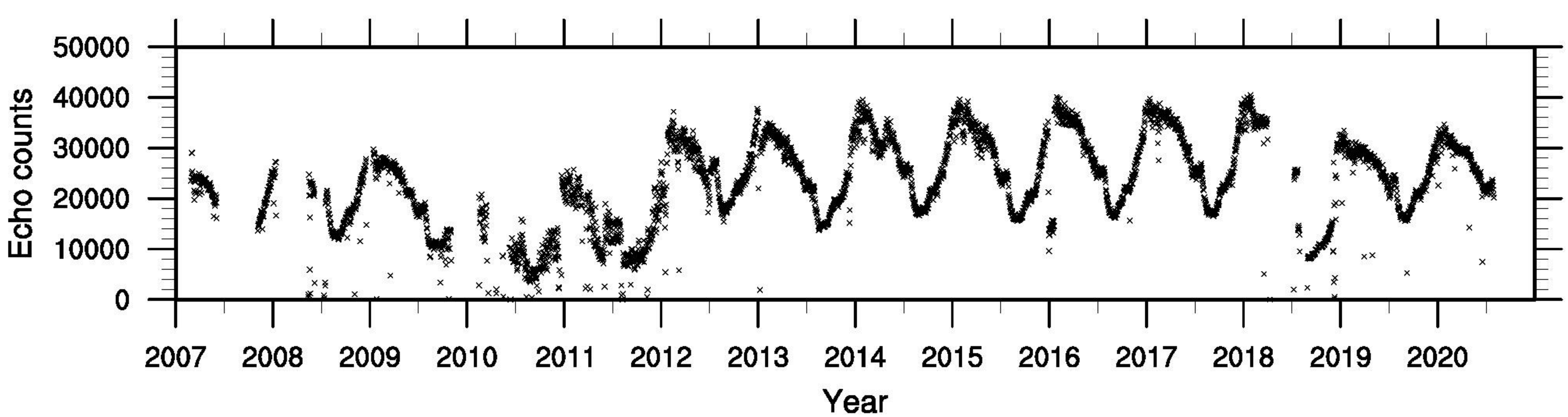

Data and Methodology (cont.)

❖ Large-scale wind components

- The fast Fourier transform (FFT) is used in each 4-day (96-hour) window incremented in 1-hour time steps. Here, we select a 4-day window to include the 2- and 4-day wave, which is somewhat large in the mesosphere.
- The large-scale wind components within the 4-day window include
  - Tidal components
    - diurnal (24 h), semidiurnal (12 h), and terdiurnal (8 h) tides
  - PW components
    - 2- and 4-day waves

❖ Temporal variations and spectral analysis

- Monthly-averaged data
  - only for months when more than 15 days of observations were conducted
- Spectral analysis
  - the Lomb-Scargle periodogram method (Lomb, 1976; Scargle, 1982) is used

Data and Methodology (cont.)

❖ MERRA-2 reanalysis data

MERRA-2 reanalysis data on model level		
Variables		*u*, *v*, *w*, *T*, and O3 mass mixing ratio
Period		2007–2020 (14 years)
Resolution	Temporal	3 hours
	Horizontal	0.625° × 0.5° (lon. x lat.)
	Vertical	72 layers (up to 0.01 hPa (~80.6 km))

- **PW propagation**: Eliassen-Palm fluxes ($F^{(\phi)}$, $F^{(z)}$)

$$F^{(\phi)} = \rho_0 a cos\phi \left[\frac{\partial \bar{u}}{\partial z} \frac{\overline{v'\theta'}}{\partial\bar{\theta}/\partial z} - \overline{u'v'} \right], \qquad F^{(z)} = \rho_0 a cos\phi \left[f_a \frac{\overline{v'\theta'}}{\partial\bar{\theta}/\partial z} - \overline{u'w'} \right].$$

- **PW generation by a baroclinic instability**: zero potential vorticity gradient ($\frac{\partial \bar{q}}{a\partial\phi} = 0$)

$$\frac{\partial \bar{q}}{a\partial\phi} \equiv \frac{2\Omega cos\phi}{a} - \frac{1}{a^2}\frac{\partial}{\partial\phi}\left[\frac{1}{cos\phi}\frac{\partial(\bar{u}cos\phi)}{\partial\phi}\right] - \frac{1}{\rho_0}\frac{\partial}{\partial z}\left(\rho_0 \frac{{f_0}^2}{N^2}\frac{\partial\bar{u}}{\partial z}\right).$$

  - ✓ The perturbation: a departure from the zonal mean

Zonal winds

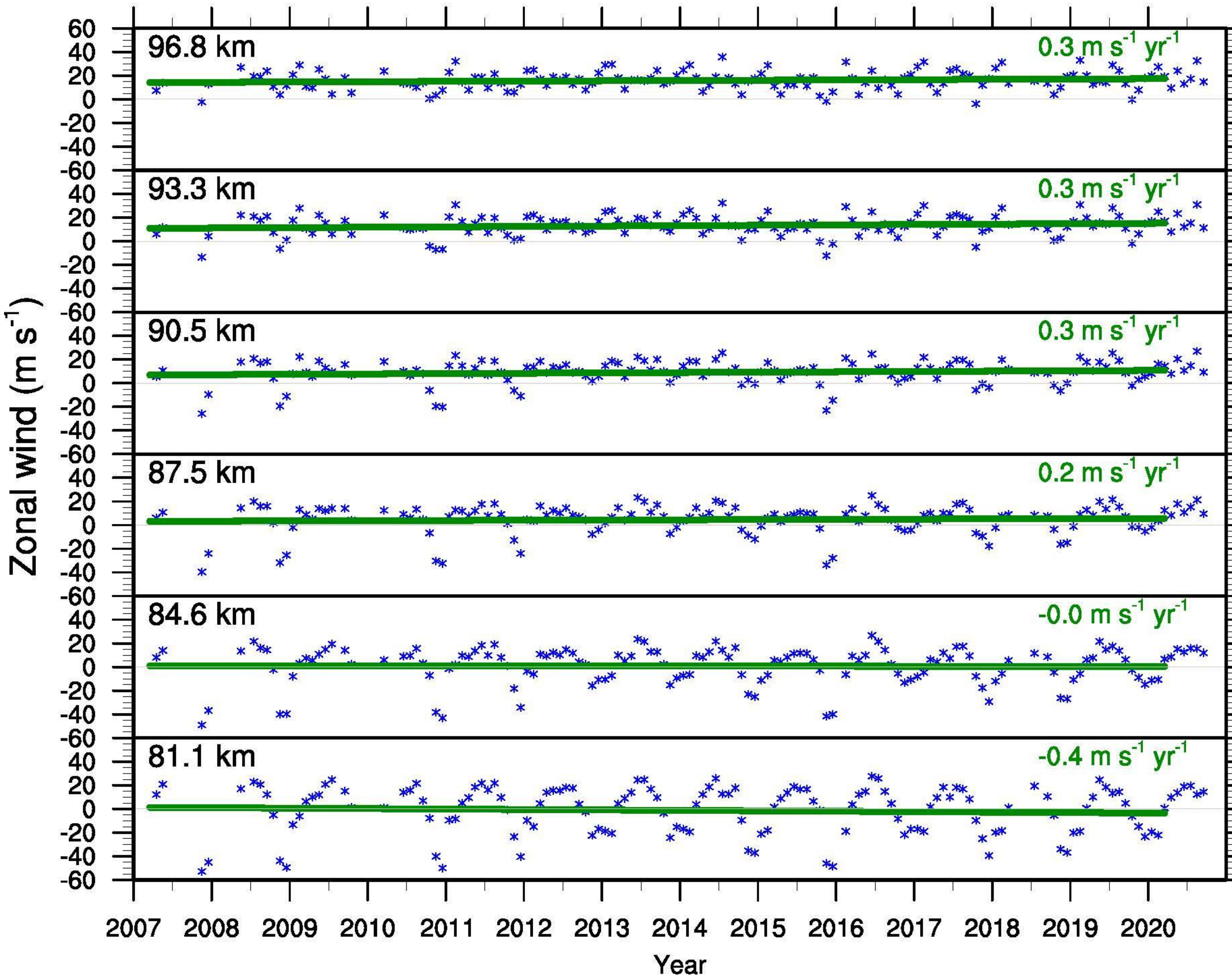

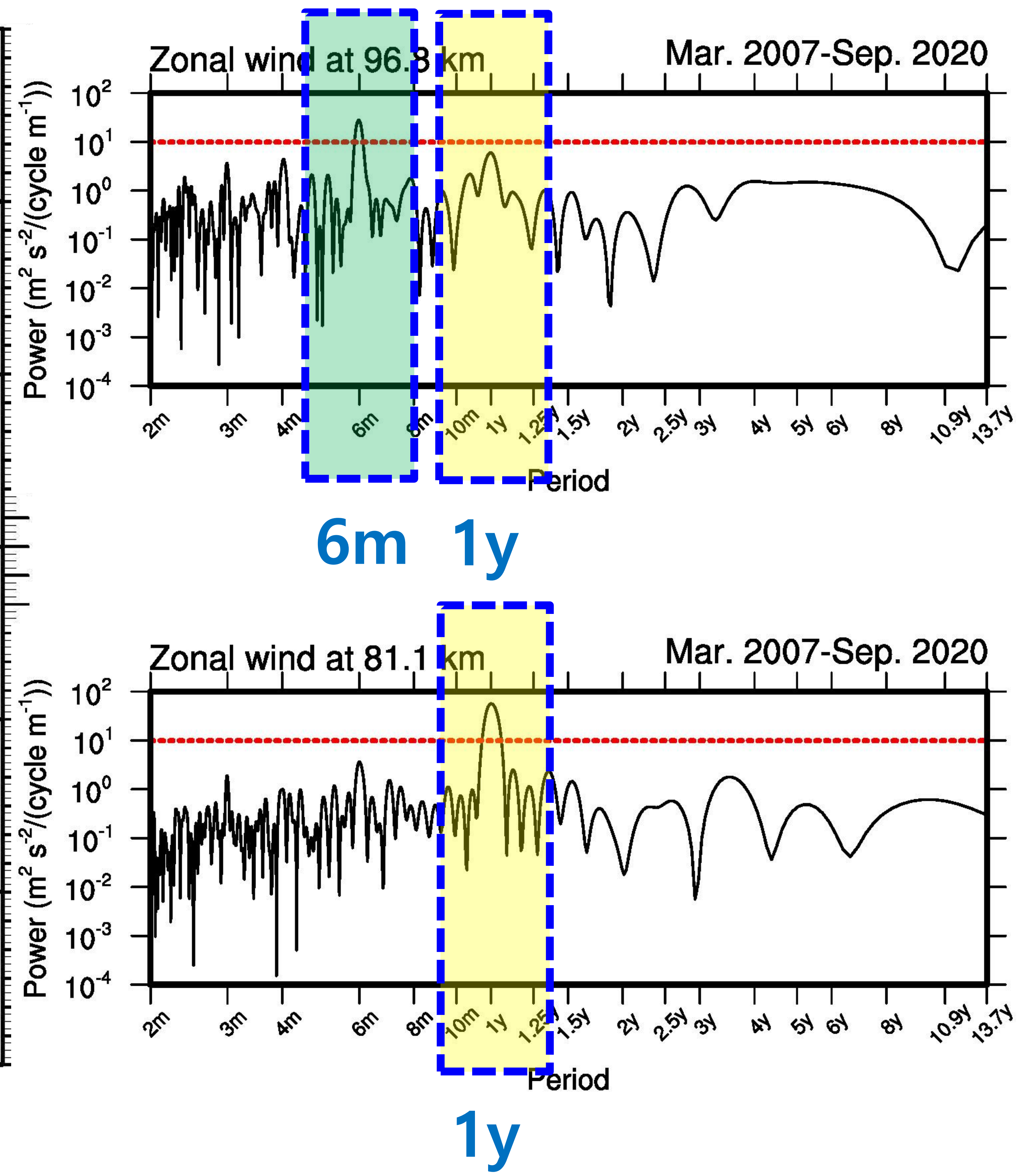

- Blue dot: monthly-averaged value, Red line: 2-month running averaged value, Green line: linear trend

- $z < 90$ km: annual variations (eastward winds in winter and westward winds in summer)
- $z > 90$ km: annual and semiannual variations
- No statistically significant linear trend is found both in monthly- and seasonally-avg. values

Meridional winds

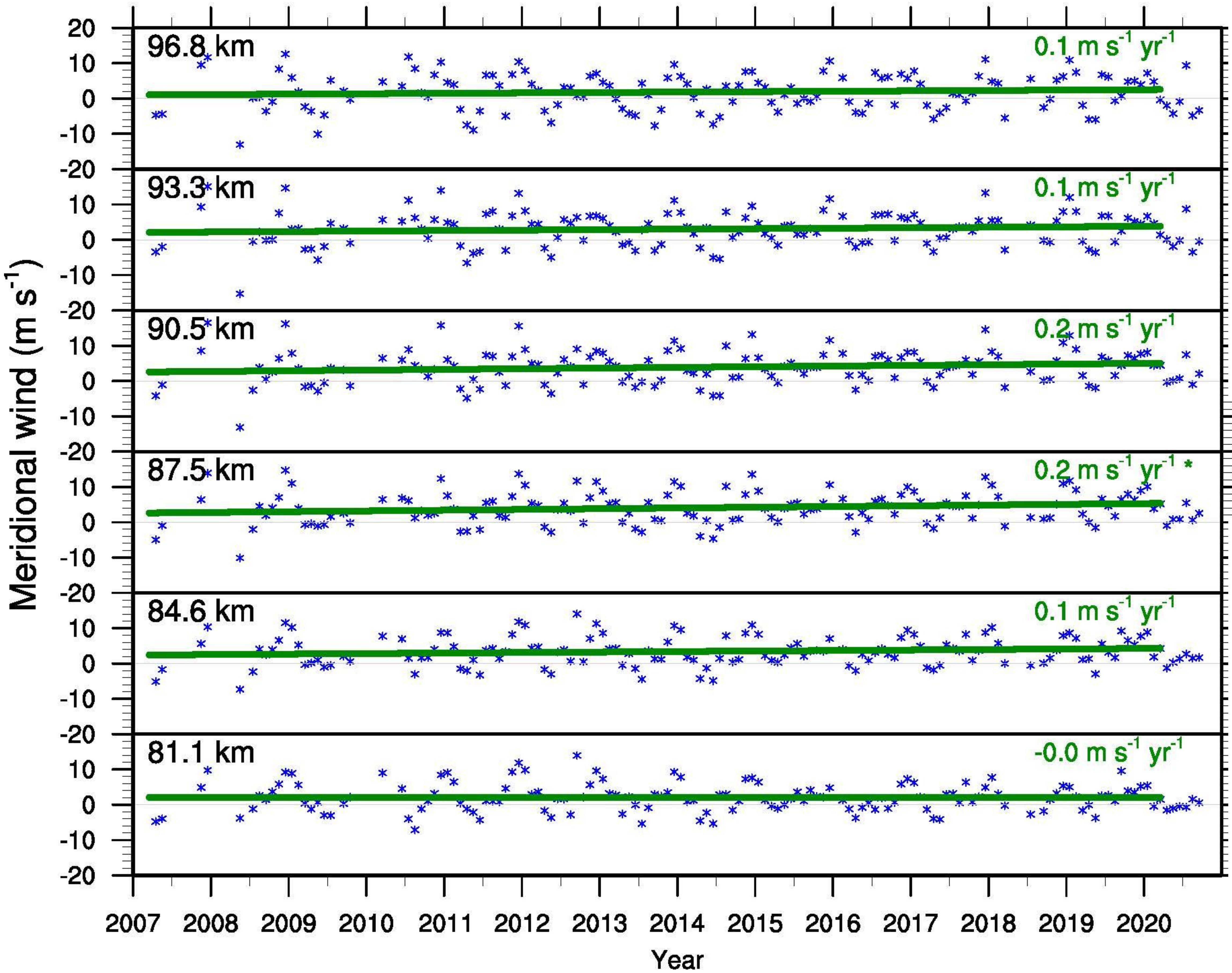

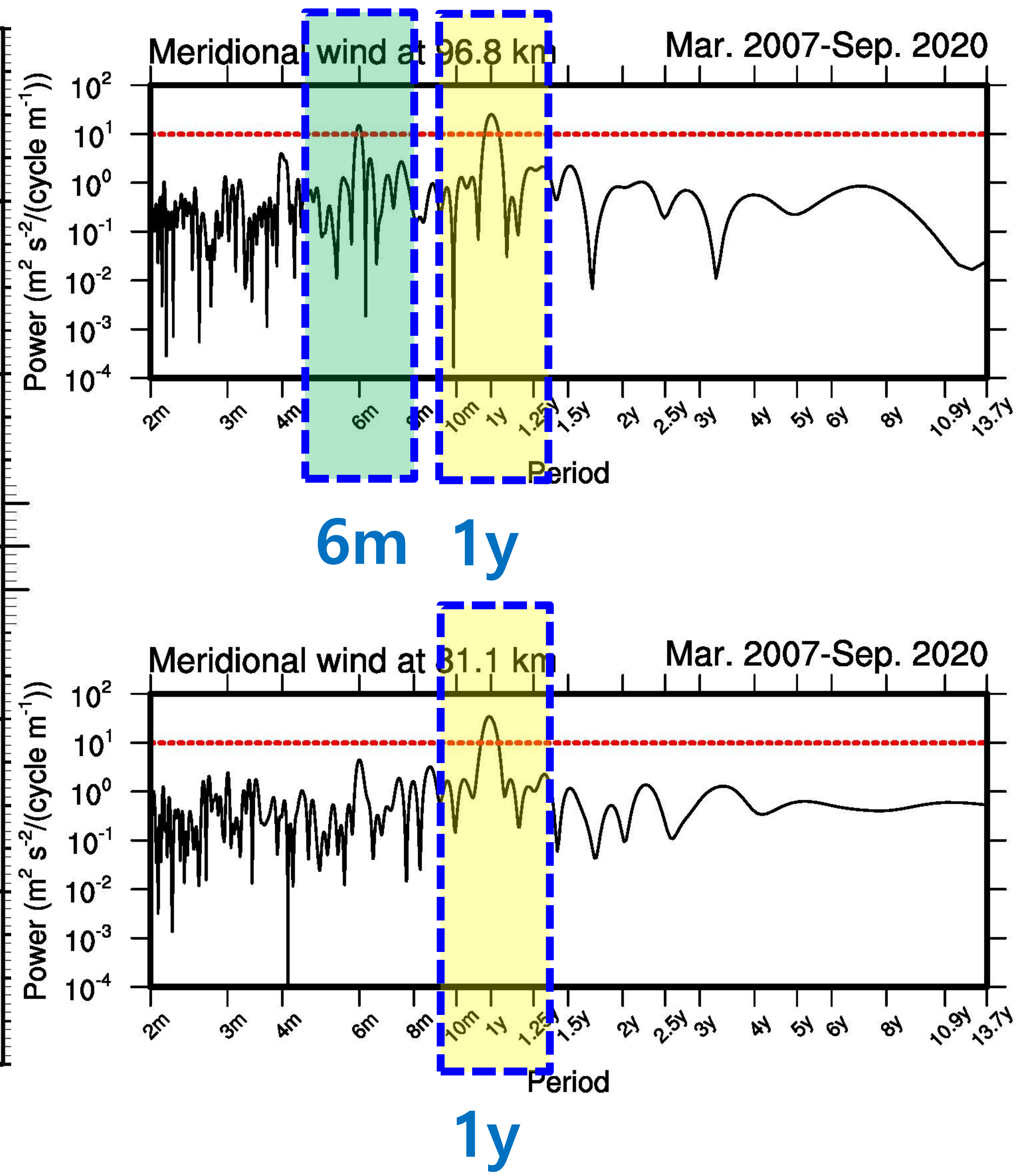

- Blue dot: monthly-averaged value, Red line: 2-month running averaged value, Green line: linear trend

- Smaller than the zonal winds
- Mostly equatorward, except in autumn
- Annual (in whole height range) and semiannual (above z = 90 km) variations
- No statistically significant linear trend

Tidal and PW components

- **Tides**: **Black**: Semidiurnal tide, **Red**: Diurnal tide, Green: Terdiurnal tide
- **PWs**: **Blue**: 2-day wave, **Gold**: 4-day wave

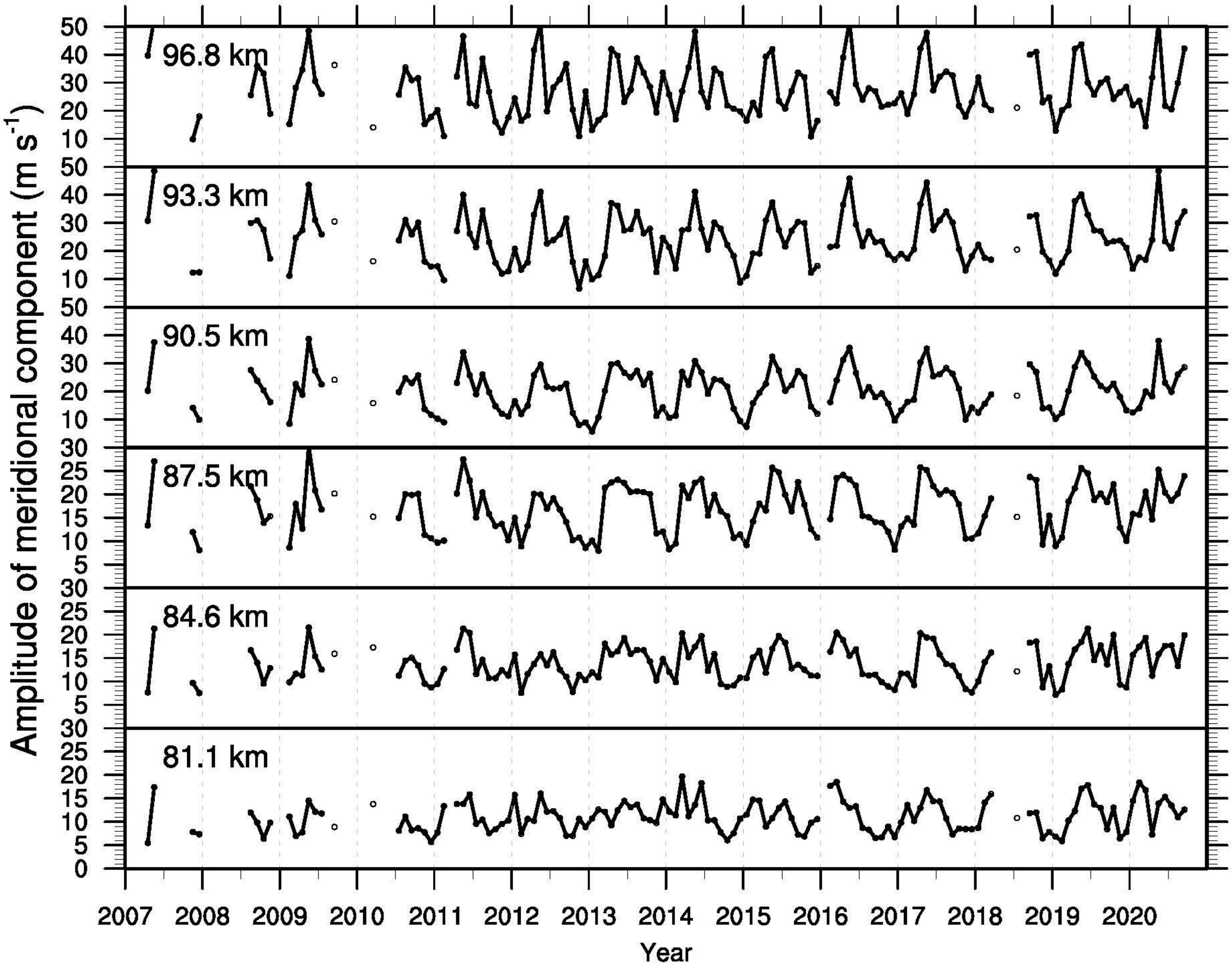

Tidal and PW components

- **Tides**: **Black**: Semidiurnal tide, **Red**: Diurnal tide, Green: Terdiurnal tide
- **PWs**: **Blue**: 2-day wave, **Gold**: 4-day wave

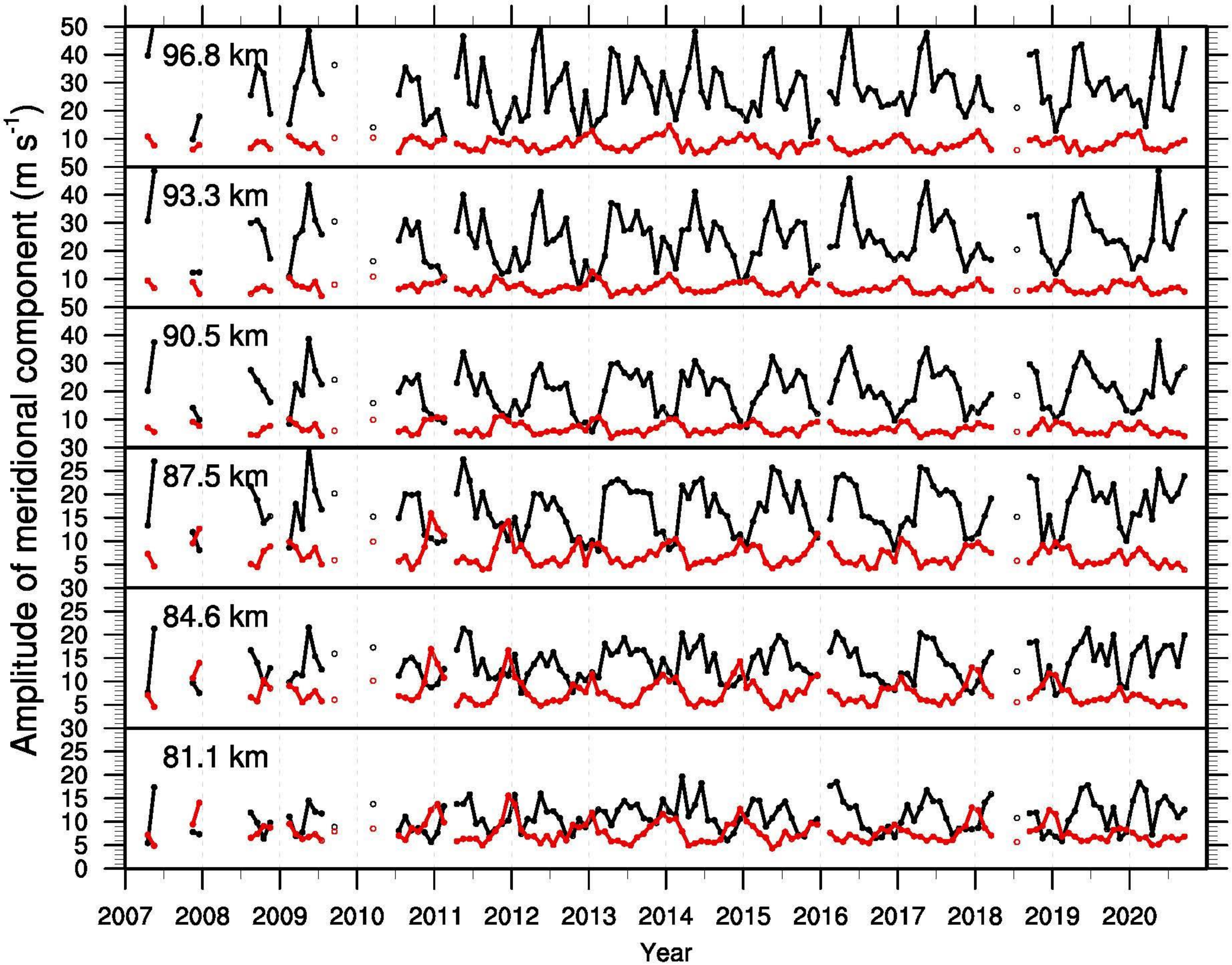

Tidal and PW components

- **Tides**: **Black**: Semidiurnal tide, **Red**: Diurnal tide, Green: Terdiurnal tide
- **PWs**: **Blue**: 2-day wave, **Gold**: 4-day wave

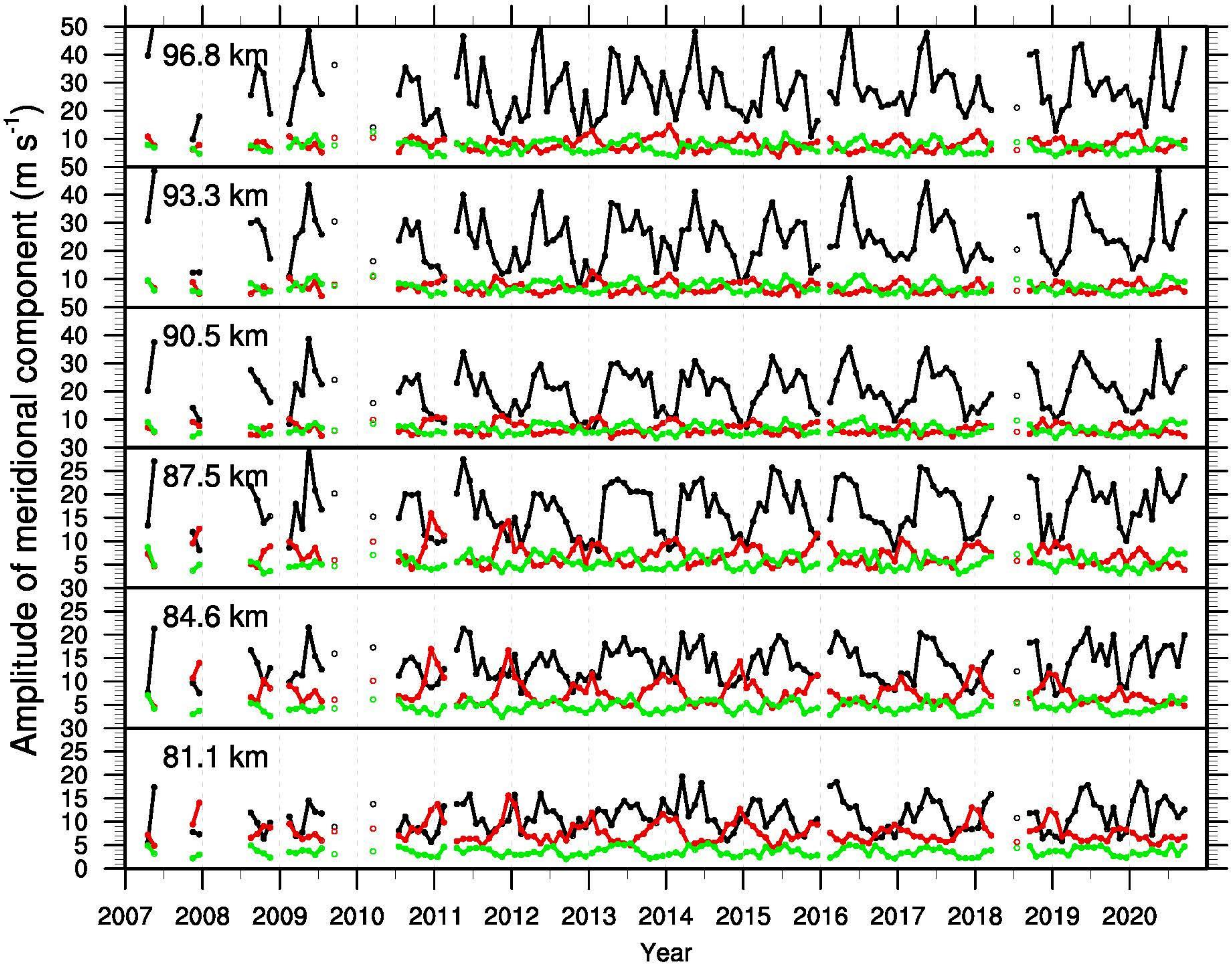

Tidal and PW components

- **Tides**: **Black**: Semidiurnal tide, **Red**: Diurnal tide, Green: Terdiurnal tide
- **PWs**: **Blue**: 2-day wave, **Gold**: 4-day wave

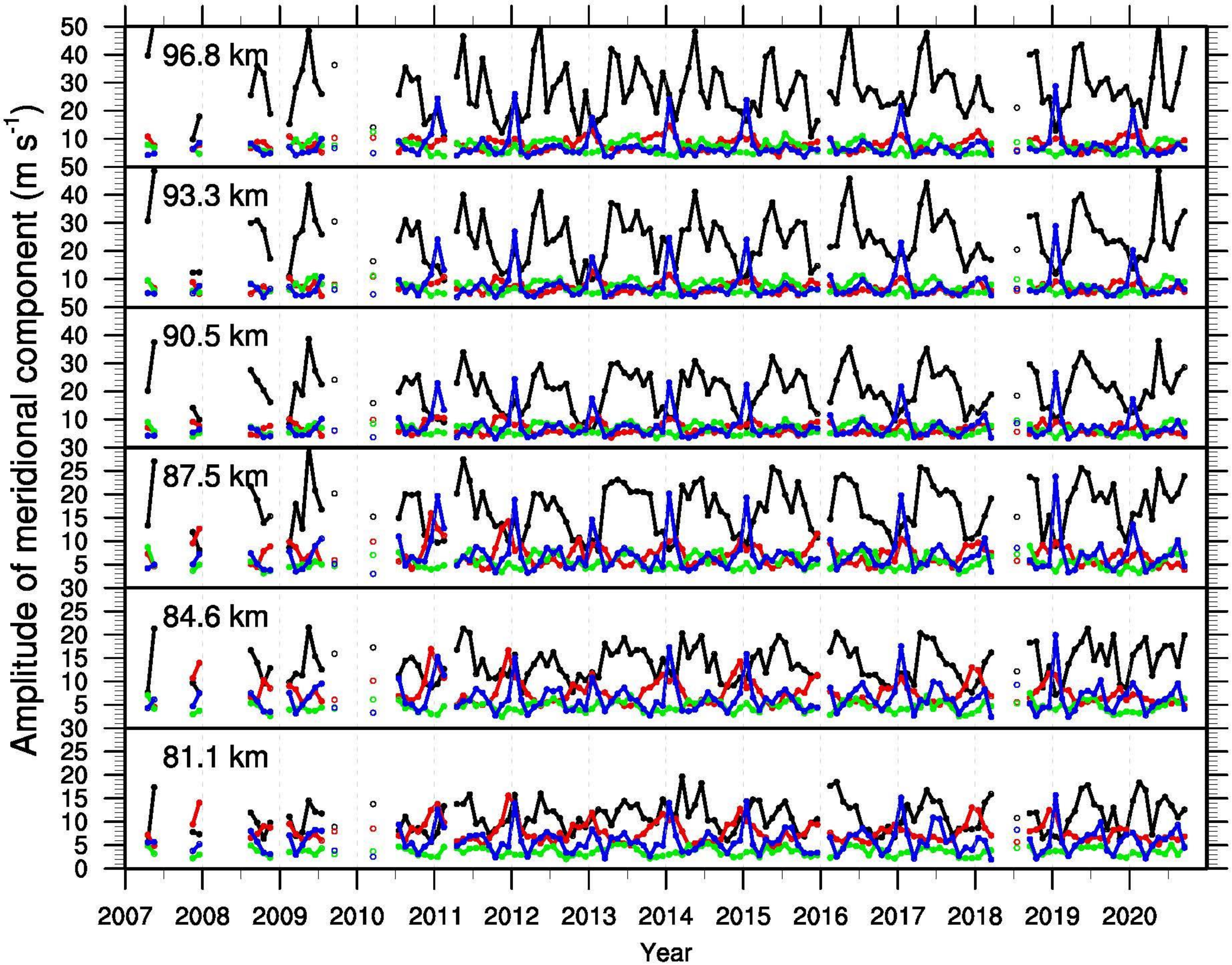

Tidal and PW components

- **Tides**: **Black**: Semidiurnal tide, **Red**: Diurnal tide, Green: Terdiurnal tide
- **PWs**: **Blue**: 2-day wave, **Gold**: 4-day wave

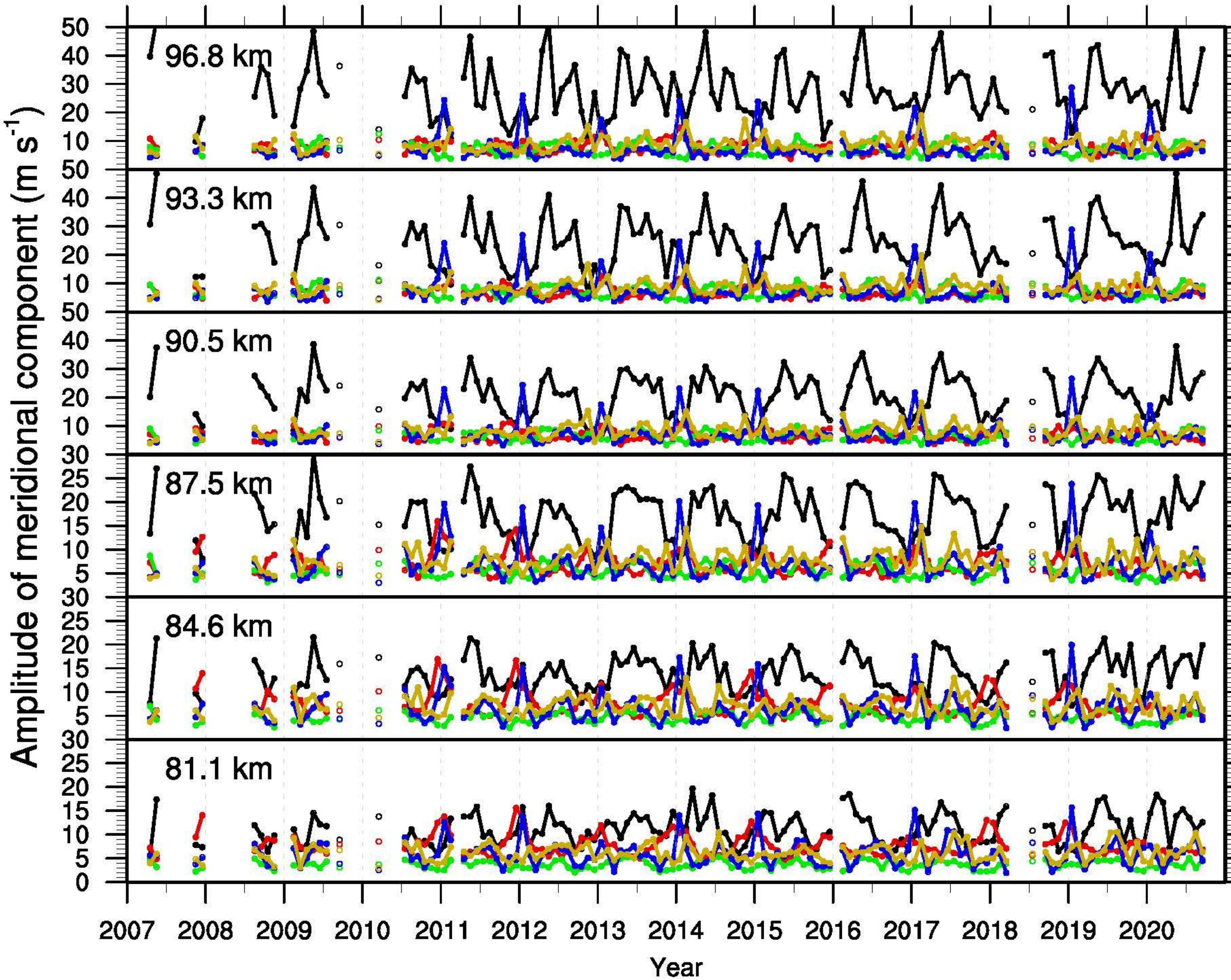

Tidal and PW components

- **Tides**: **Black**: Semidiurnal tide, **Red**: Diurnal tide, Green: Terdiurnal tide
- **PWs**: **Blue**: 2-day wave, **Gold**: 4-day wave

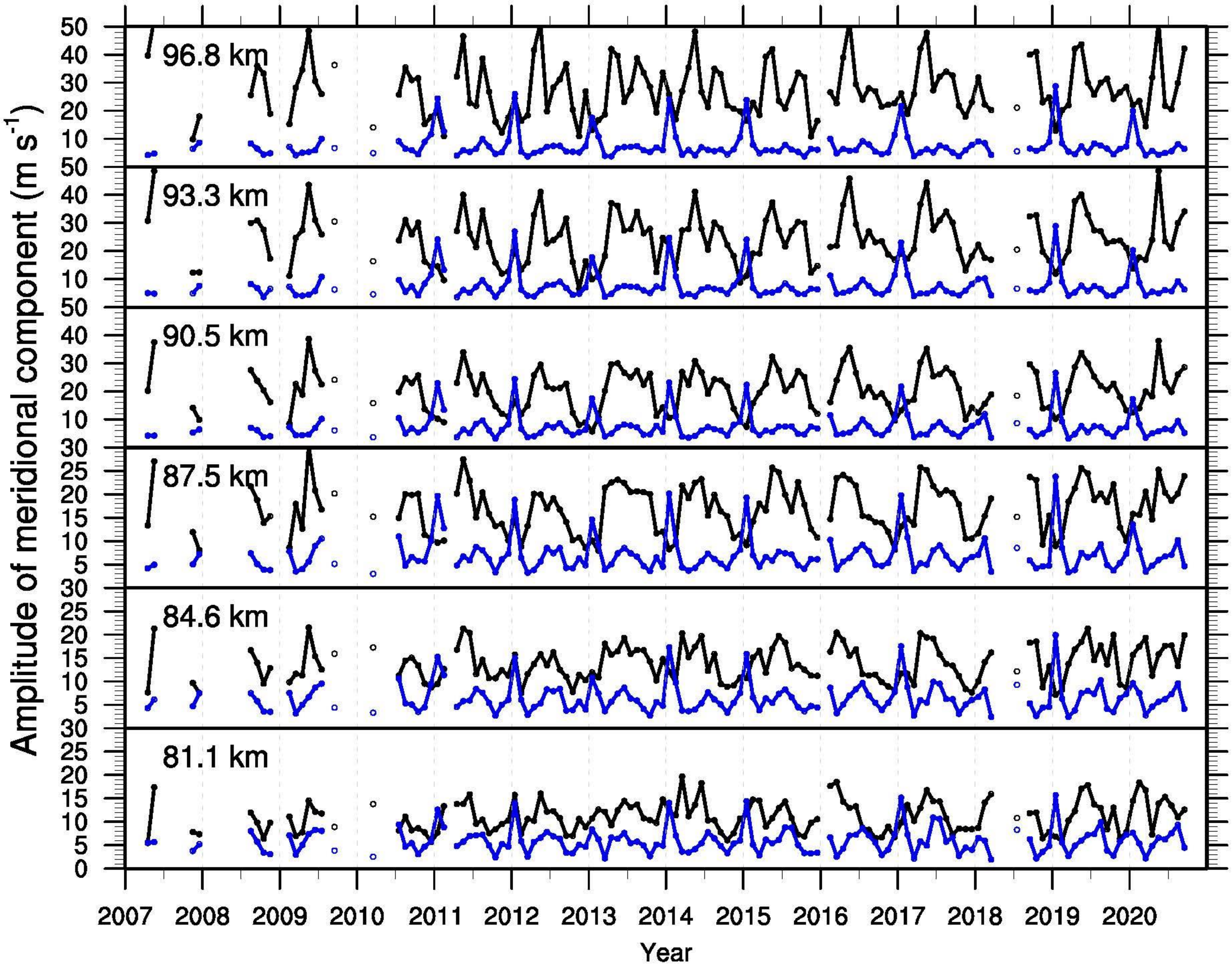

Semidiurnal tides

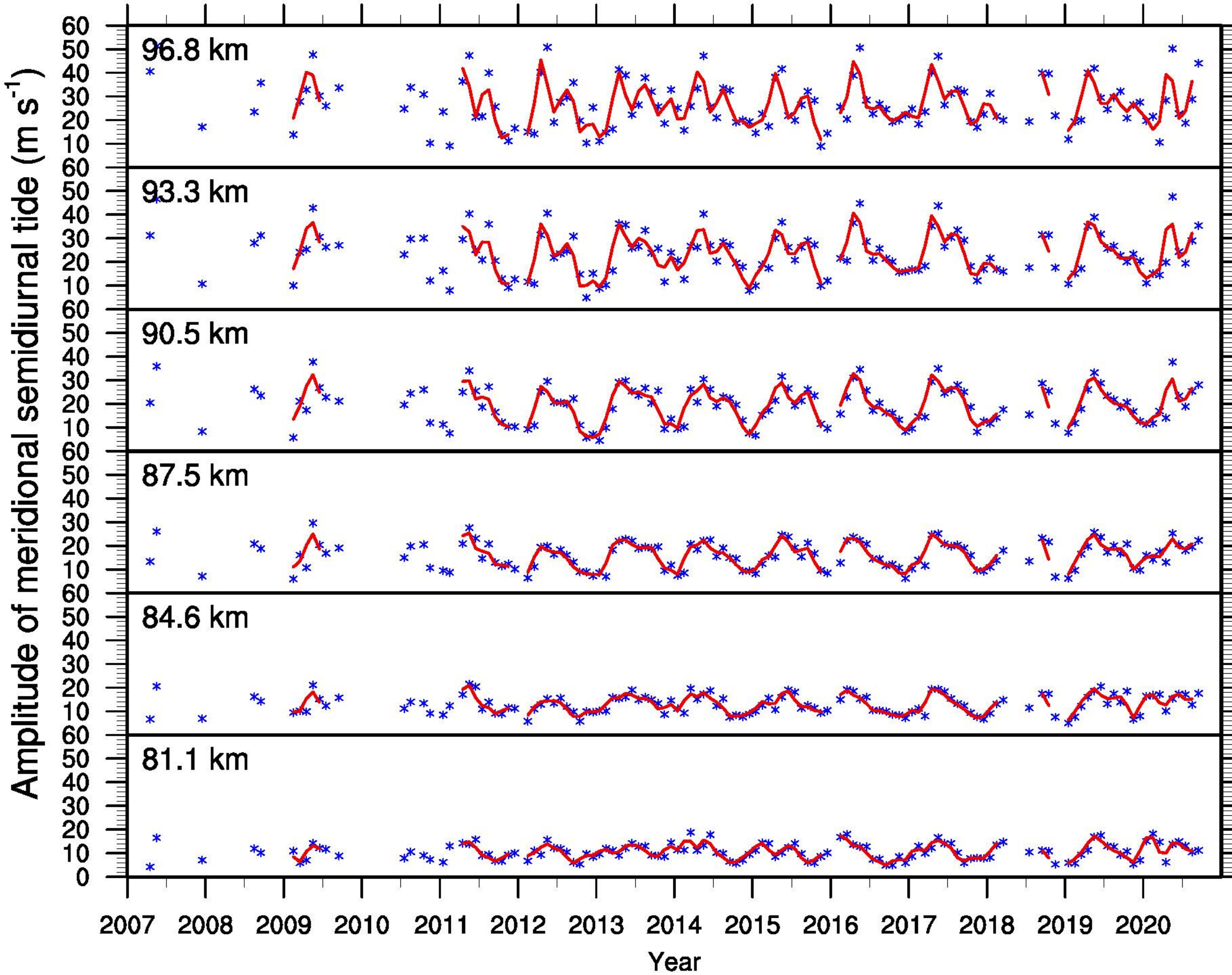

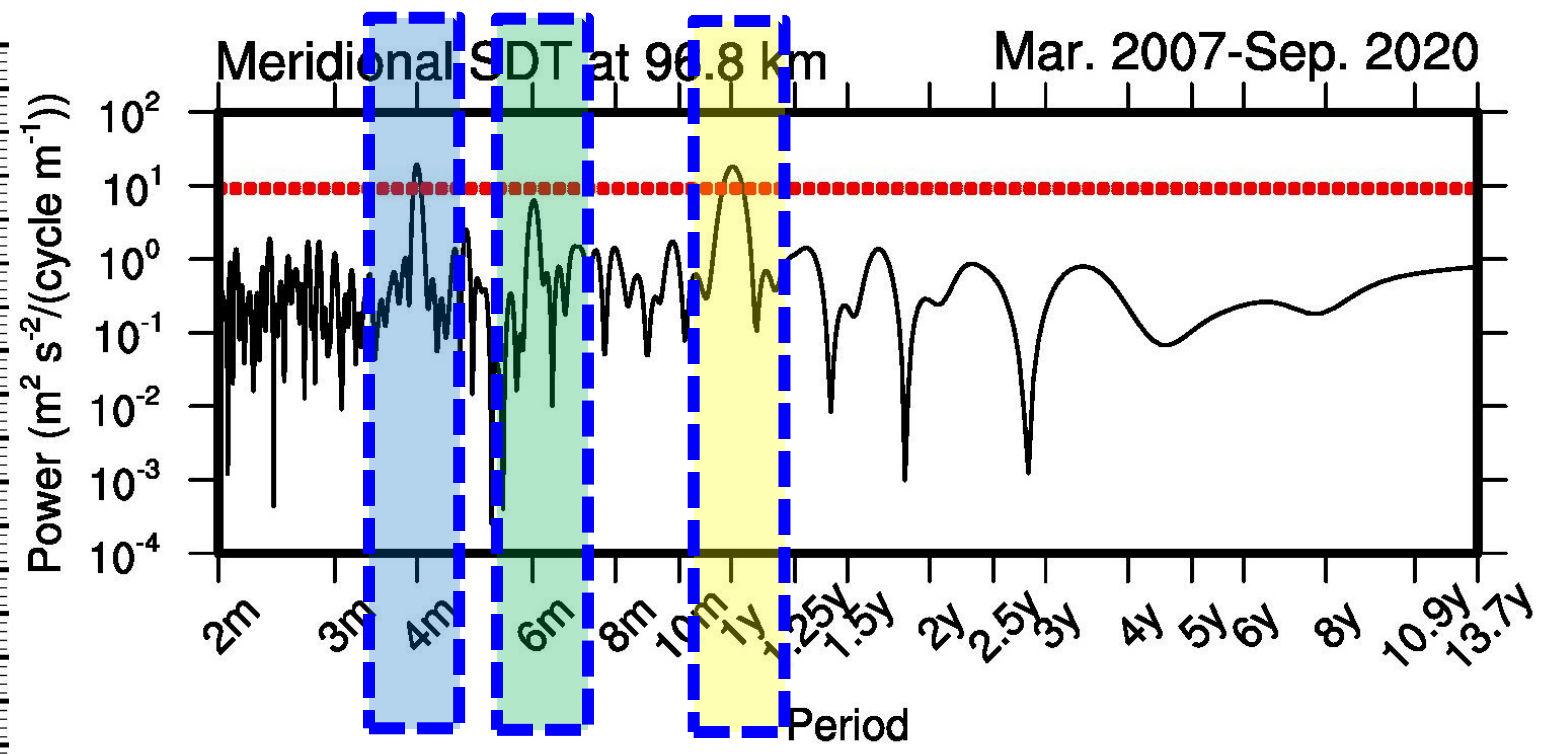

4m 6m 1y

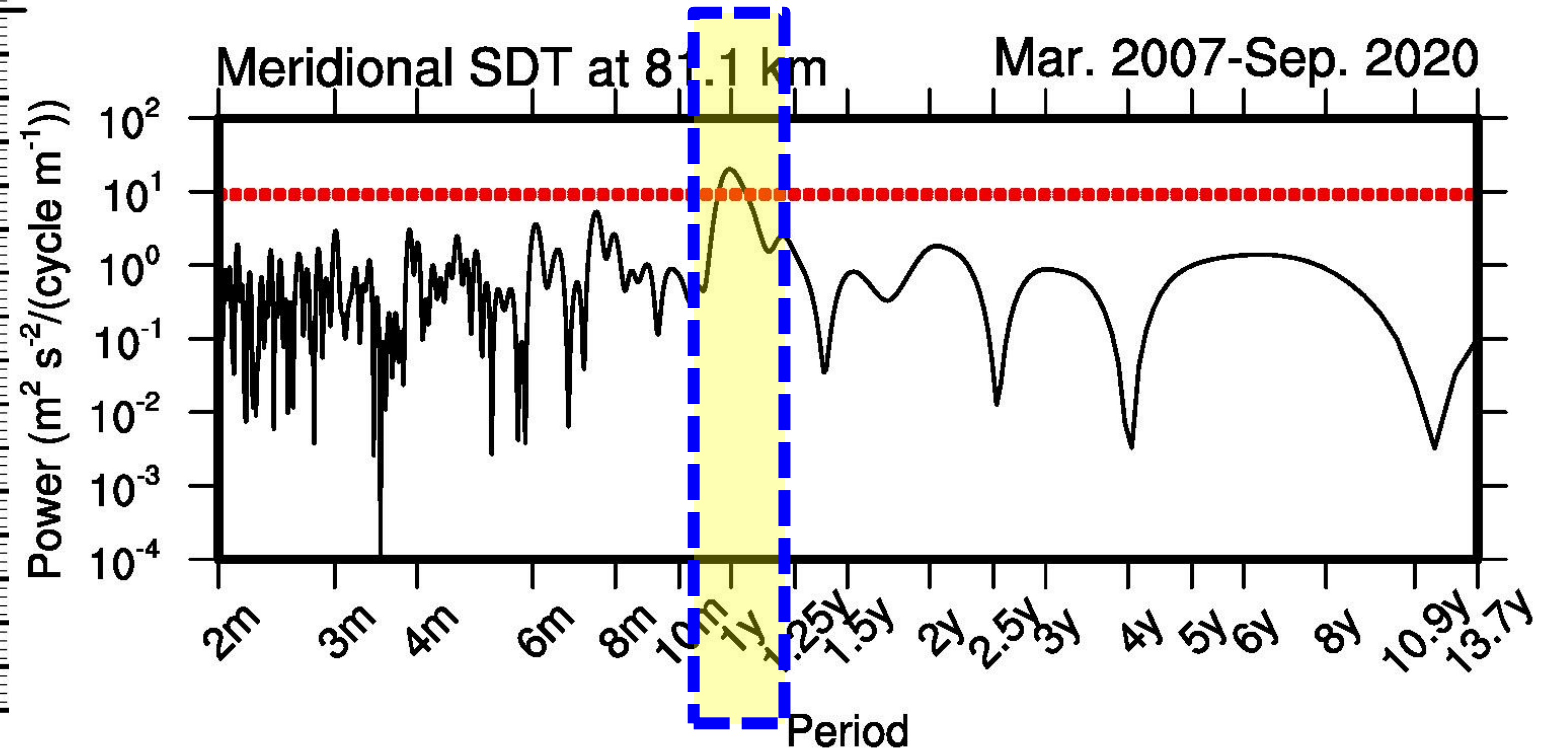

1y

- Blue dot: monthly-averaged value, Red line: 2-month running averaged value, Green line: linear trend

- The growth of the amplitude of semidiurnal tides with height
- Annual, semiannual, and terannual variations with a primary peak in May

Semidiurnal tides and stratospheric ozone mixing ratio

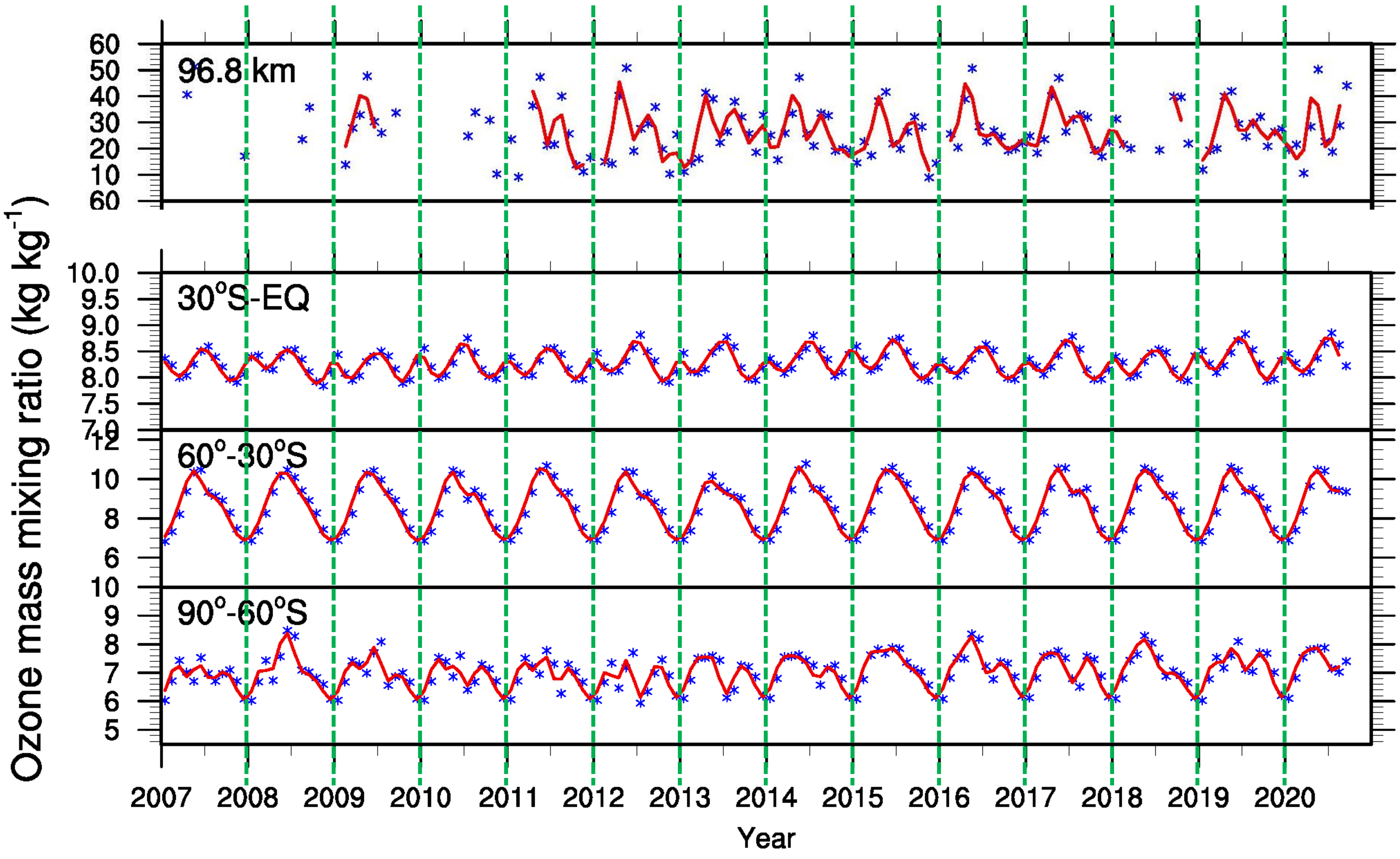

- The semidiurnal tide is generated by the interaction of solar radiation with stratospheric ozone
- No significant linear trends are found both in amplitude of SDT and ozone mixing ratio, except for increasing trends in amplitude of SDT above 93.3 km during spring (not shown)

2-day waves

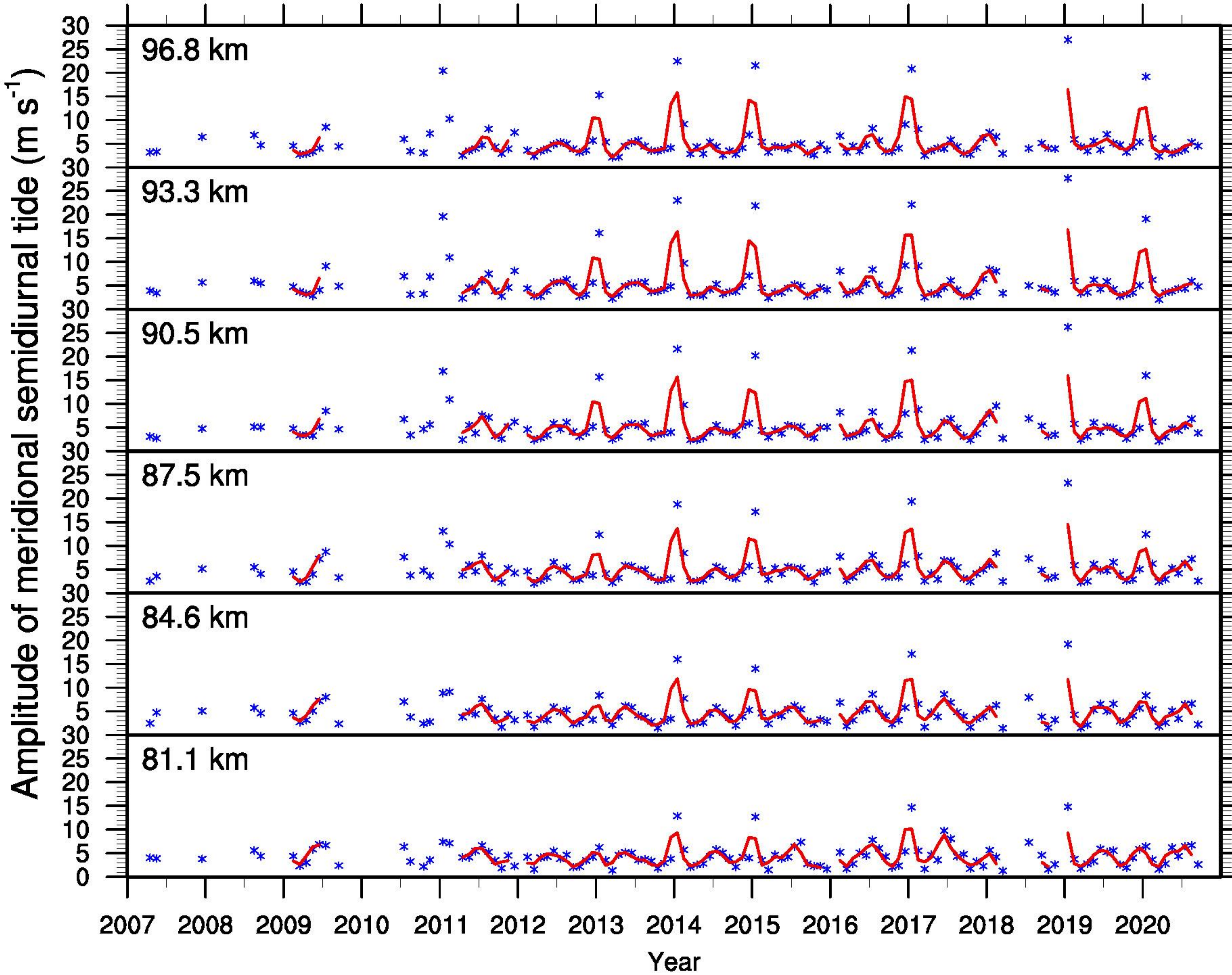

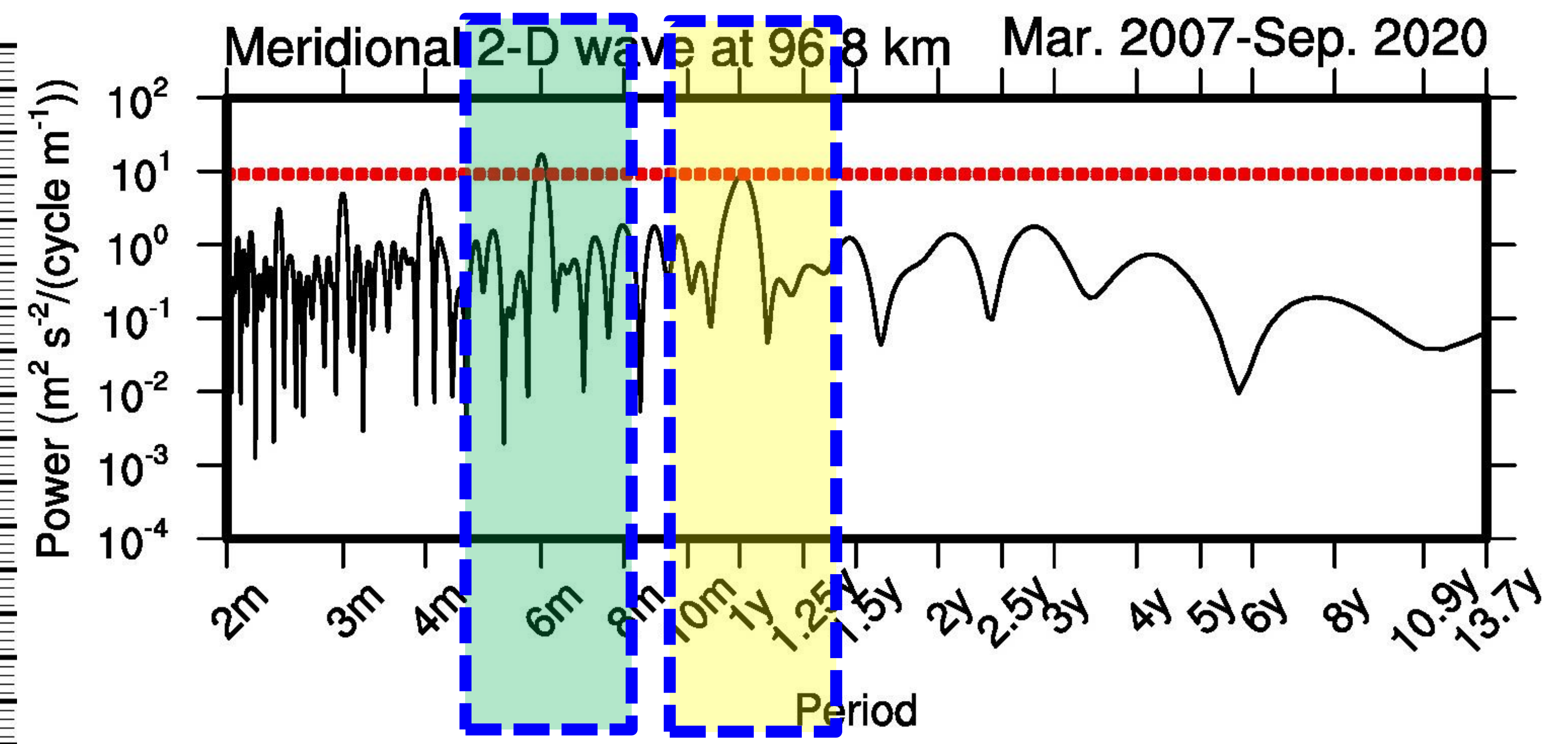

6m 1y

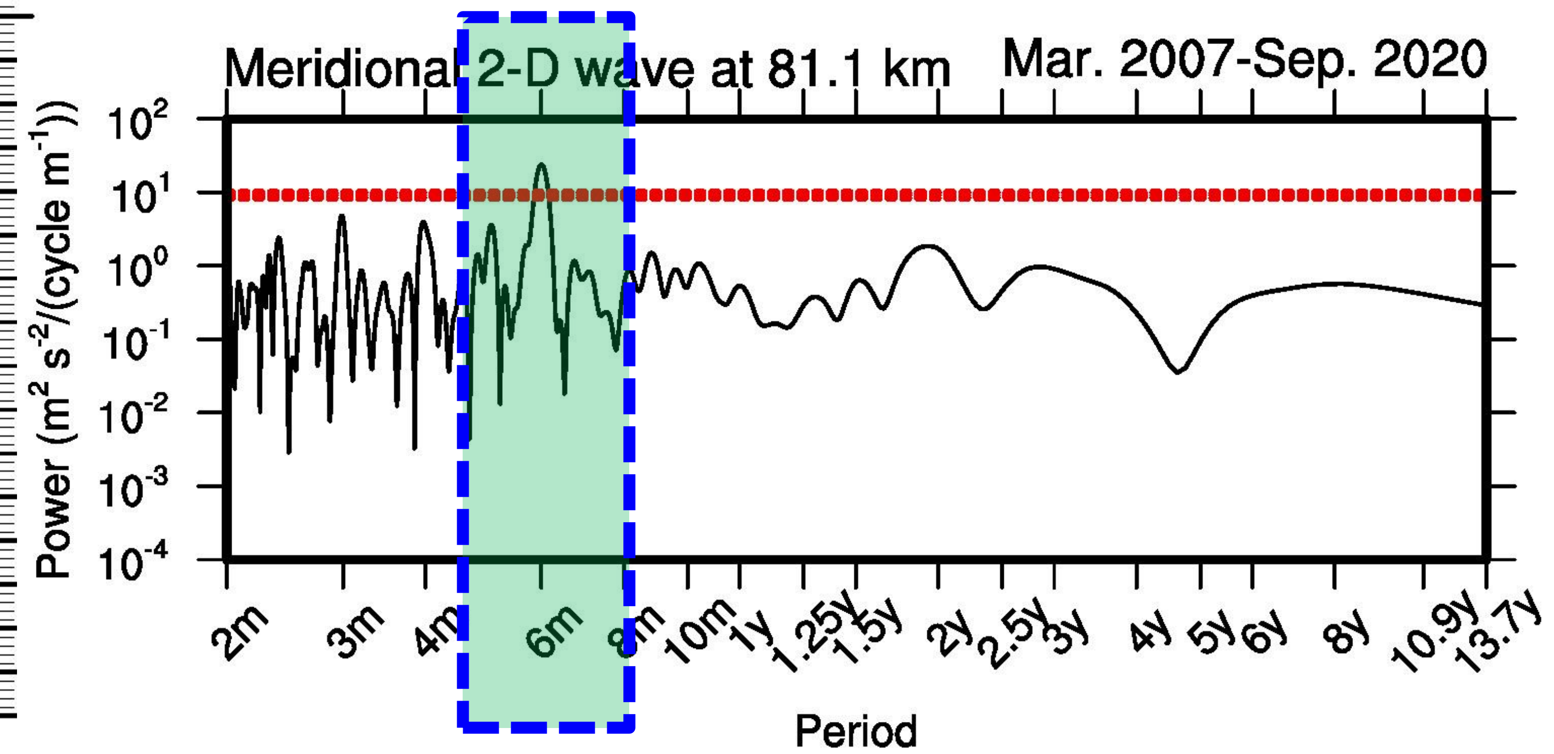

6m

- Blue dot: monthly-averaged value, Red line: 2-month running averaged value, Green line: linear trend

- Annual and semiannual variations with a primary peak in January
- No statistically significant linear trend

Generation and propagation of the 2-day waves in

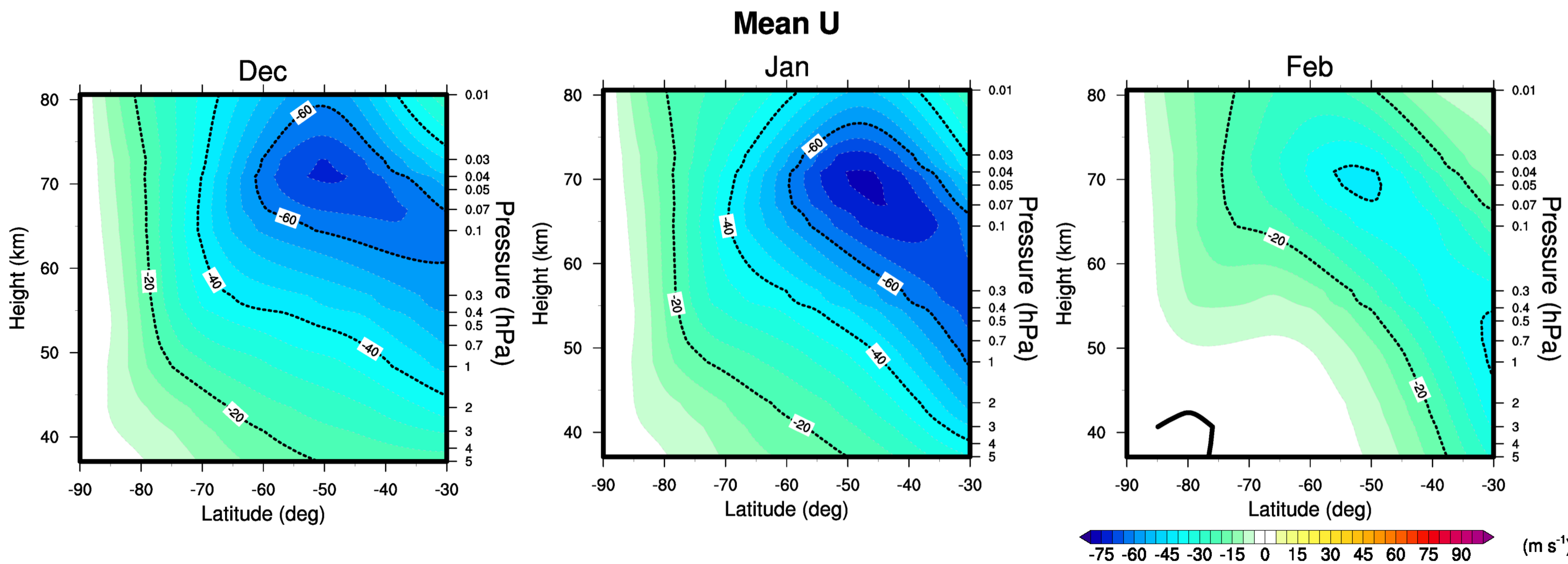

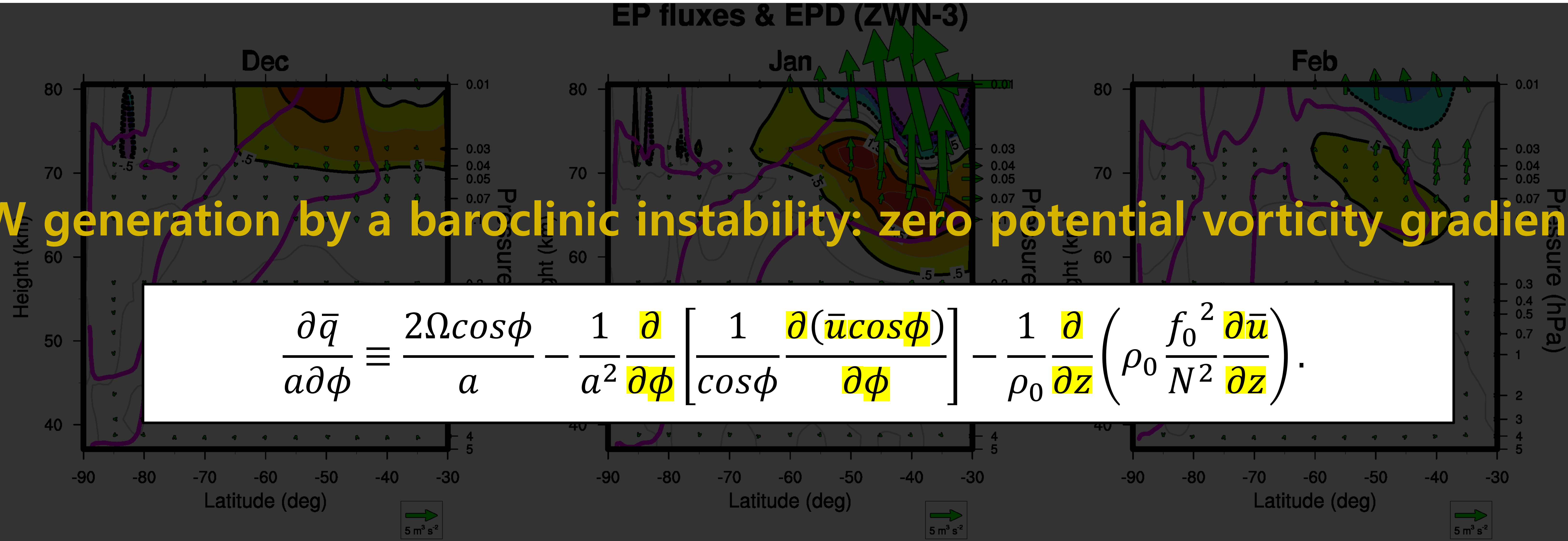

PW generation by a baroclinic instability: zero potential vorticity gradient

$$\frac{\partial \bar{q}}{a\partial\phi} \equiv \frac{2\Omega cos\phi}{a} - \frac{1}{a^2}\frac{\partial}{\partial\phi}\left[\frac{1}{cos\phi}\frac{\partial(\bar{u}cos\phi)}{\partial\phi}\right] - \frac{1}{\rho_0}\frac{\partial}{\partial z}\left(\rho_0\frac{{f_0}^2}{N^2}\frac{\partial\bar{u}}{\partial z}\right).$$

- **Vector**: Eliassen-Palm flux, **shading**: EP flux divergence,
- Magenta contour: zero PV gradient line

Summary and discussions

- **Meteor radar** at **KSS** in the Antarctic Peninsula are used to analyze **winds in the MLT** region over a **14-year** period (2007–2020).
  - Annual and semiannual variations in horizontal winds are observed in MLT region.
  - No statistically significant linear trends are found.
- Spectral analysis of the observed horizontal winds is performed to investigate the characteristics of **tides** and **planetary waves**
  - Amplitude of the **semidiurnal tide** is the largest among the three tidal component.
  - The semidiurnal tidal signal is dominant above 90 km, especially in May, which has also been shown in previous studies (Hibbins et al., 2007; Lee et al., 2013).
  - Strong semidiurnal tide activities are associated with the **ozone** concentration in the **stratosphere** over mid- and high-latitudes.
  - The amplitude of the **2-day wave** shows clear seasonal variability, with a maximum value in summer (especially in January), secondary maximum in winter, and near-zero value in spring and autumn, which is consistent with previous studies (Baumgaertner et al., 2008; Manson et al., 2004; Murphy et al., 2007; Nozawa et al., 2003; Phillips, 1989; Sandford et al., 2008; Tunbridge & Mitchell, 2009).
  - In January, the 2-day wave generated by the **baroclinic instability** in the mid-latitude upper stratosphere can propagate to the MLT in the polar regions.

THANK YOU.

Fig. 4

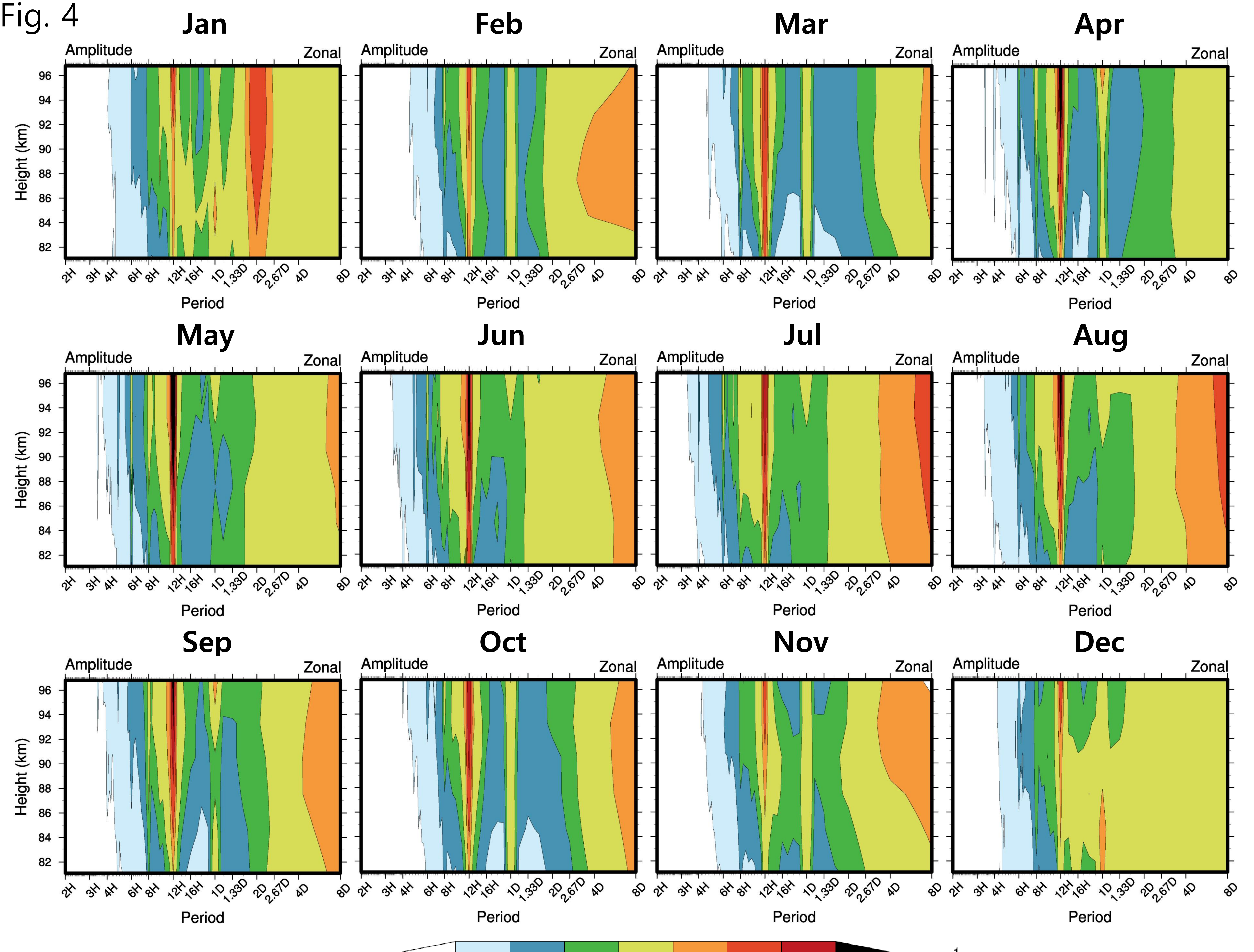

Jan
Feb
Mar
Apr
May
Jun
Jul
Aug
Sep
Oct
Nov
Dec
Amplitude
Zonal
Height (km)
96
94
92
90
88
86
84
82
2H
3H
4H
6H
8H
12H
16H
1D
1.33D
2D
2.67D
4D
8D
Period

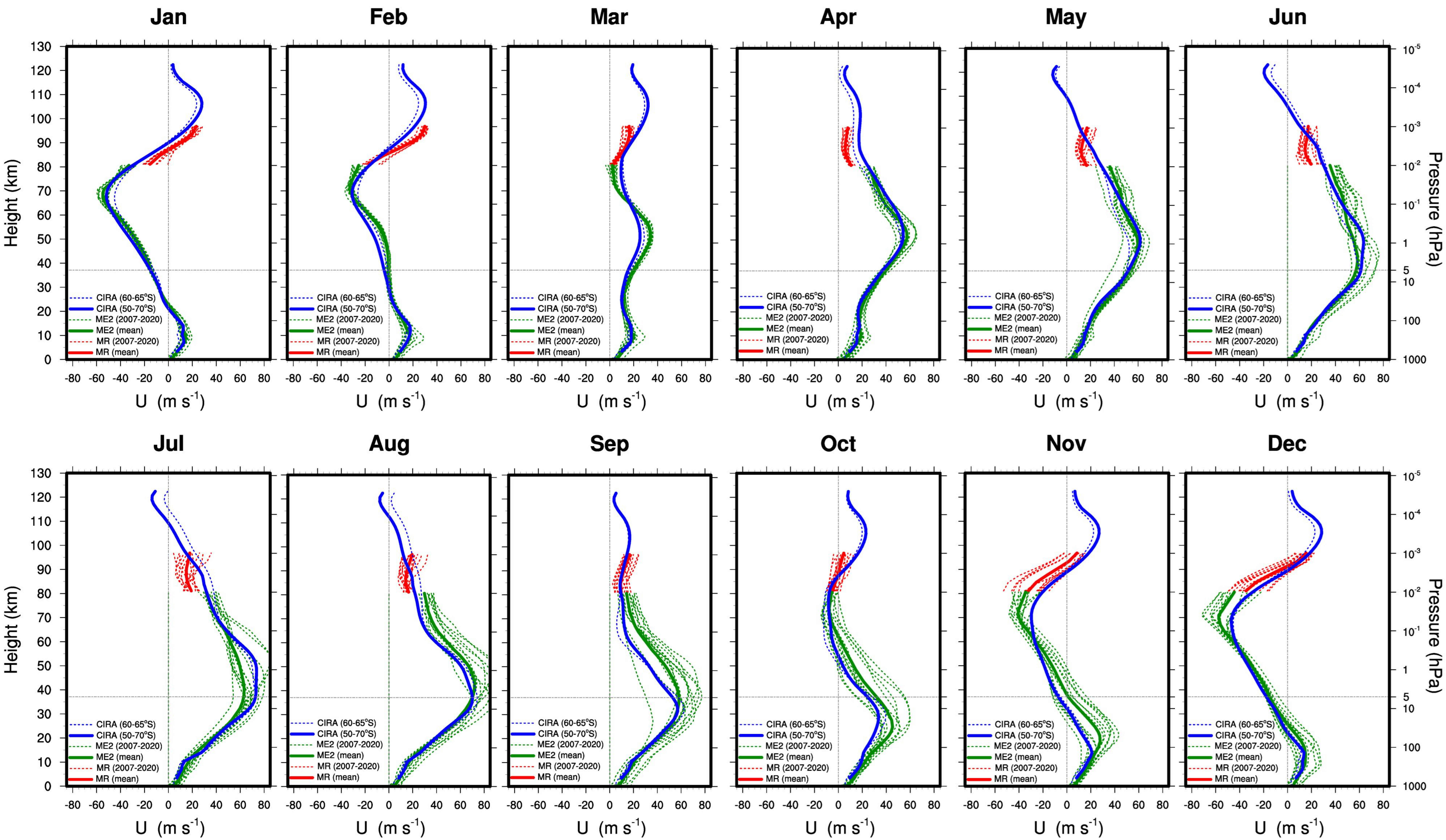
Jan
Feb
Mar
Apr
May
Jun
Jul
Aug
Sep
Oct
Nov
Dec
Height (km)
Pressure (hPa)
U (m s^{-1})
CIRA (60-65°S)
CIRA (50-70°S)
ME2 (2007-2020)
ME2 (mean)
MR (2007-2020)
MR (mean)

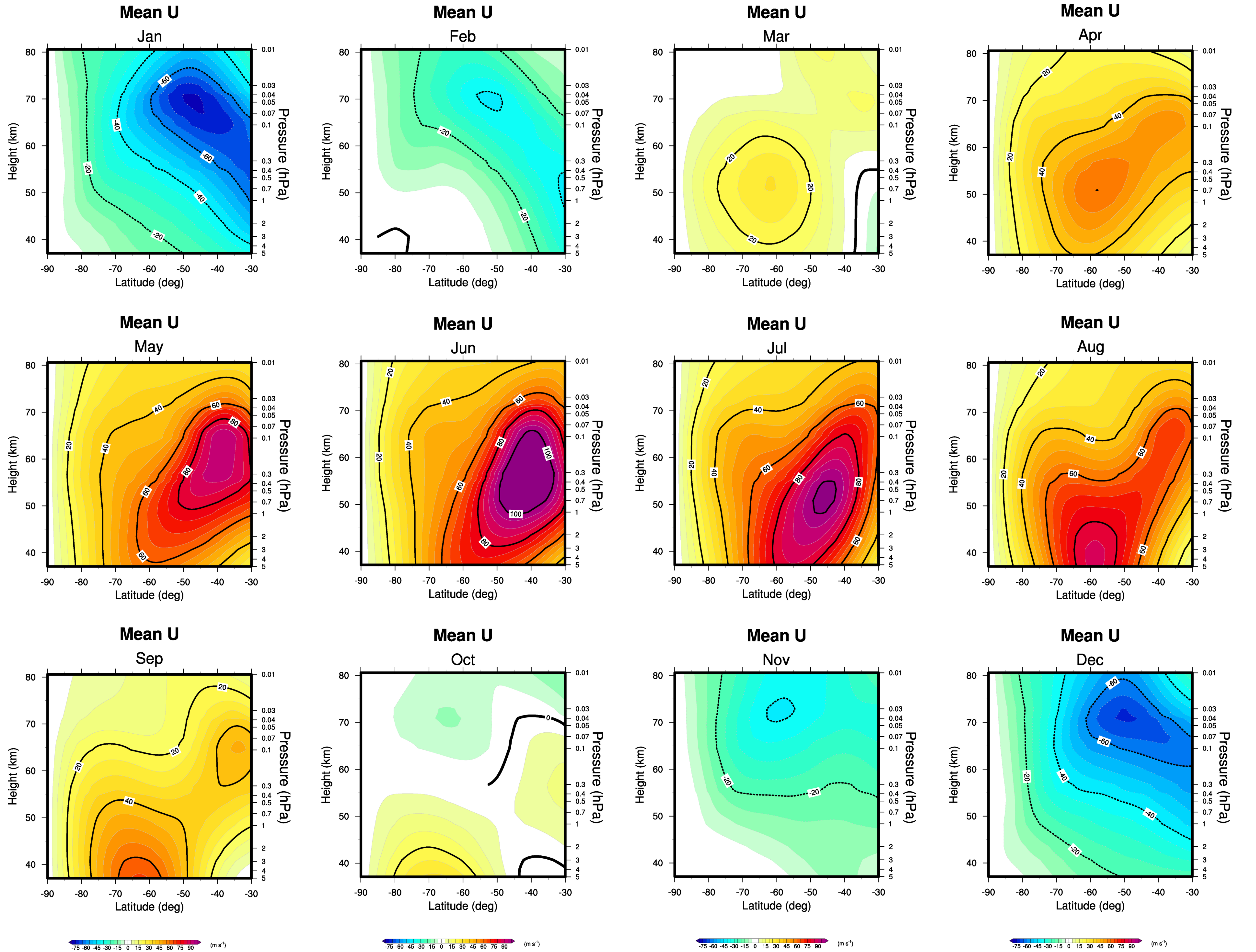

Mean U
Jan
Mean U
Feb
Mean U
Mar
Mean U
Apr
Mean U
May
Mean U
Jun
Mean U
Jul
Mean U
Aug
Mean U
Sep
Mean U
Oct
Mean U
Nov
Mean U
Dec
Height (km)
Pressure (hPa)
Latitude (deg)
-90 -80 -70 -60 -50 -40 -30
40 50 60 70 80
0.01 0.03 0.04 0.05 0.07 0.1 0.3 0.4 0.5 0.7 1 2 3 4 5
-75 -60 -45 -30 -15 0 15 30 45 60 75 90
(m s-1)

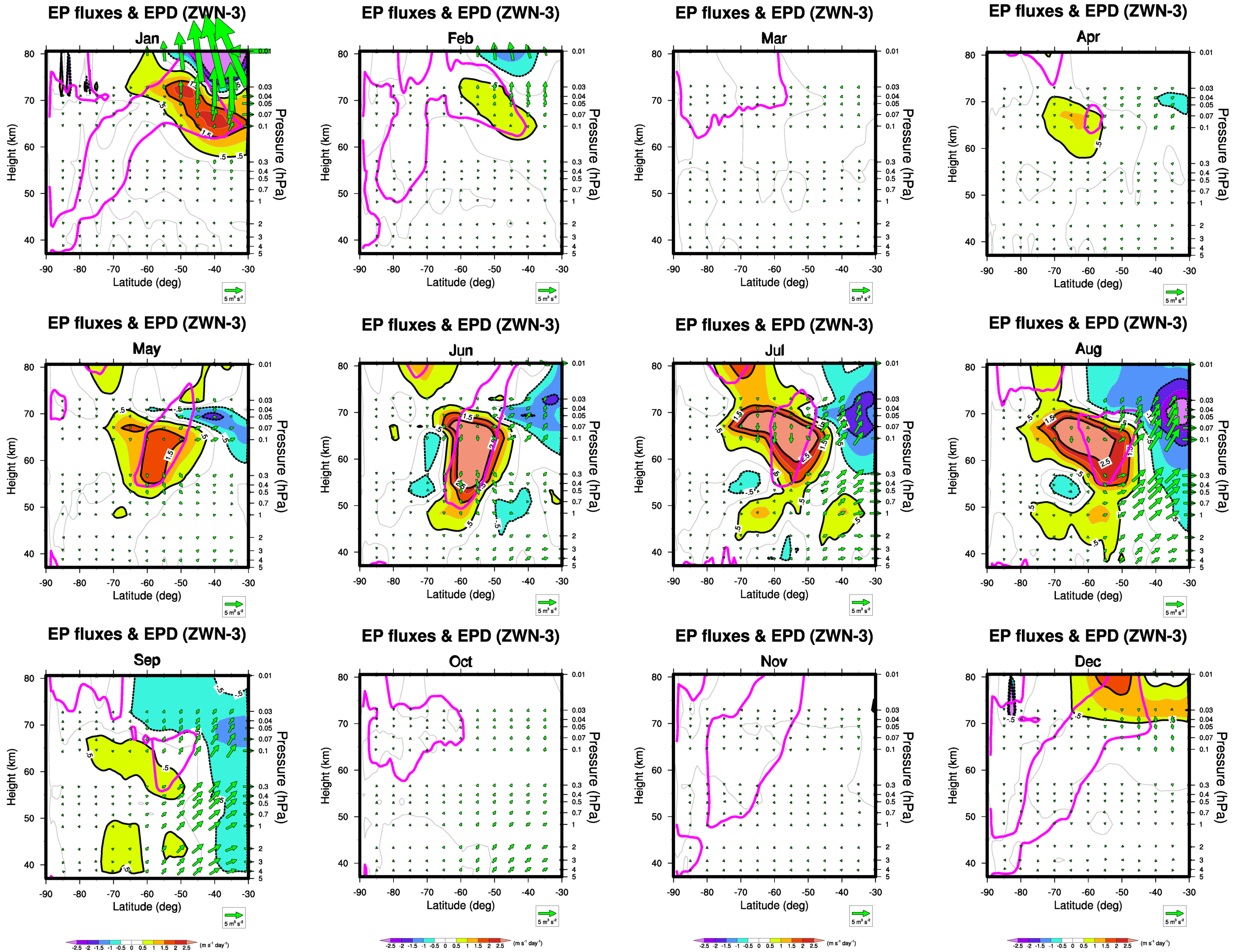
EP fluxes & EPD (ZWN-3)
Jan
Feb
Mar
Apr
May
Jun
Jul
Aug
Sep
Oct
Nov
Dec
Height (km)
Pressure (hPa)
Latitude (deg)
5 m³ s⁻²
-2.5 -2 -1.5 -1 -0.5 0 0.5 1 1.5 2 2.5
(m s⁻¹ day⁻¹)